arXiv:1701.03520v1 [cond-mat.soft] 11 Jan 2017

Ring closure in actin polymers

Supurna Sinha [1] and Sebanti Chattopadhyay [2]

[1] *Raman Research Institute, Bangalore 560080, India.*
[2] *Doon University, Dehradun 248001, India.*

(Dated: January 16, 2017)

We present an analysis for the ring closure probability of semiflexible polymers within the pure bend Worm Like Chain (WLC) model. The ring closure probability predicted from our analysis can be tested against fluorescent actin cyclization experiments.We also discuss the effect of ring closure on bend angle fluctuations in actin polymers.

PACS numbers: 87.15.Cc,62.20.de,82.35.-x,87.10.-e

I. INTRODUCTION

In the past two decades, there has been much interest in the theoretical study of semiflexible polymer elasticity. These studies are motivated by micromanipulation experiments[1–3] on biopolymers. In particular, in recent years there have been experiments involving stretching DNA molecules[1] which give us information about the bend elastic properties of DNA. There have also been experiments on fluorescently tagged actin filaments[4] where they measure the bend persistence length of actin. More recently, there have been fluorescence experiments on cyclization of actin filaments[5]. In these papers they analyze the formation of rings in actin polymers and study the effect of ring closure on bend angle fluctuations in these polymeric rings. Our interest here is limited to the process of cyclization itself and therefore in our analysis we restrict to polymers with only bend degrees of freedom and no twist degree of freedom. Actin cyclization is of interest to biologists [6] who do visualization studies of actin ring formation in the context of cell division.

II. RING CLOSURE PROBABILITY DISTRIBUTION

Our starting point is the pure bend Worm Like Chain (WLC) model[7]. In this model, the polymer configuration is viewed as a space curve $\vec{x}(s)$. There is a tangent vector associated with each point on the polymer of contour length L and the energy of configuration is given by:

$$\mathcal{E}[\mathcal{C}] = \frac{A}{2}\int_0^L ds\kappa^2 \tag{1}$$

where $\mathcal{C}$ stands for the polymer configuration. A is the bending elastic constant and the curvature $\kappa = |\frac{d\hat{t}}{ds}|$.

One of the key quantities characterizing the elasticity of a biopolymer is $\tilde{Q}(\vec{r})$, the probability distribution for the end to end distance vector $\vec{r}$ between the two ends of the polymer as it gets jiggled around by thermal fluctuations in a cellular environment [7]. In [7] we use a method for solving the wormlike chain model for semiflexible polymers to any desired accuracy over the entire range of polymer lengths to determine $\tilde{Q}(\vec{r})$. The plots for $\tilde{Q}(\vec{r})$ for various $\beta = \frac{L}{L_P}$, the ratio of the contour length L to the persistence length L_P, reveal the dependence of the end to end distance vector on the rigidity of the polymer (See Fig. [4] in [7]).

We outline the theoretical calculation of $\tilde{Q}(\vec{r})$ below. (For a detailed exposition please see Appendix A). Consider a situation where the initial and final tangent vectors ($\hat{t}_A = \frac{d\vec{x}}{ds}|_{s=0}$ and $\hat{t}_B = \frac{d\vec{x}}{ds}|_{s=L}$) are held fixed. Then $\tilde{Q}(\vec{r})$ has the following path integral representation:

$$\tilde{Q}(\vec{r}) = \mathcal{N}\int \mathcal{D}[\hat{t}(s)]exp\{-\frac{1}{k_BT}[\frac{A}{2}\int_0^L (\frac{d\hat{t}}{ds})^2 ds]\} \times\delta^3(\vec{r}-\int_0^L \hat{t}ds) \tag{2}$$

Here $\mathcal{N}$ is the normalization constant and k_BT, the thermal energy at temperature T. As mentioned in [7], we solve for $\tilde{Q}(\vec{r})$ by first considering a related end to end distance measure:

$$P(z) = \int d\vec{r}\tilde{Q}(\vec{r})\delta(r_3 - z),$$

which is $\tilde{Q}(\vec{r})$ integrated over a plane of constant z. This in turn is related to $\tilde{P}(f)$, the Laplace transform of $P(z)$ given by:

$$\tilde{P}(f) = \int_{-L}^{L} P(z)e^{\frac{fz}{L_P}}dz \tag{3}$$

f, the variable conjugate to z has the interpretation of a stretching force and thus $\tilde{P}(f)$, can be written as the ratio $Z(f)/Z(0)$ of the partition functions in the presence and absence of an external stretching force f. We do an eigenspectrum analysis of $\tilde{P}(f)$ and determine $\tilde{Q}(\vec{r})$ using tomographic transformations outlined in [7].

Here we address a question which is of current interest to application of polymer physics to biology: cyclization of actin filaments[5]. Within the pure bend Worm Like Chain (WLC) Model we compute the ring closure probability (RCP) by considering $\tilde{Q}(\vec{r} = \vec{0})$.

III. METHOD

In Fig. 4 of [7] we display a family of curves of $Q(\rho)$ versus ρ, with $\rho = \frac{|\vec{r}|}{\beta}$ for various values of β. $Q(\rho)$ is a theoretically convenient quantity expressed in terms of scaled units ($\vec{\rho} = \frac{\vec{r}}{\beta}$). In order to compute the ring closure probability density $\tilde{Q}(\vec{r} = \vec{0})$ we need to change variables from $\rho = \frac{|\vec{r}|}{\beta}$ to $|\vec{r}| = r$. Setting $\tilde{Q}(\vec{r}) = Q_{\vec{r}}$, we get:

$$\int Q(\vec{\rho}) d\vec{\rho} \; = \; \int Q_{\vec{r}} d\vec{r} \tag{4}$$

or

$$\int \frac{Q(\vec{\rho})}{\beta^3} d\vec{r} \; = \; \int Q_{\vec{r}} d\vec{r} \tag{5}$$

which in turn implies

$$\frac{Q(0)}{\beta^3} \; = \; Q_0 \tag{6}$$

We compute $Q(0)$ for a range of values of β using Mathematica. As we can see from the plot of the ring closure probability density $Q(0)$ versus β (Fig. 1), that $Q(0)$ has a small value for short polymers which are hard to bend and form rings and it has a large value for long polymers which are easy to bend and thus the probability density of ring formation is high. We then compute and plot the ring closure probability density in physical space, $Q_0 = \frac{Q(0)}{\beta^3}$ as a function of β (Fig. 2). The qualitative features of the plot shown in Fig. 2 are in agreement with our intuition. The ring closure probability density Q_0 in physical space, which is an experimentally measurable quantity is small for very short and long strands of the polymer and peaks around intermediate contour lengths of $L \approx 3L_P$ (See Fig. 7-41 on page 438 of [8]).

IV. MEAN SQUARED TANGENT ANGLE FLUCTUATION

One of the experimentally relevant quantities of interest is the mean squared tangent angle fluctuation[5]. In Ref. [5] the mean squared tangent angle fluctuation has been calculated for a ring and a linear filament in a two dimensional setup. They find good agreement with experimental measurements.

Here we present a similar calculation in a three dimensional geometry. Consider a polymer configuration in a closed circular ring lying in the $x-y$ plane. Expanding the bend angle fluctuation $\phi(s)$ in a Fourier series and imposing the ring closure constraint and removing zero

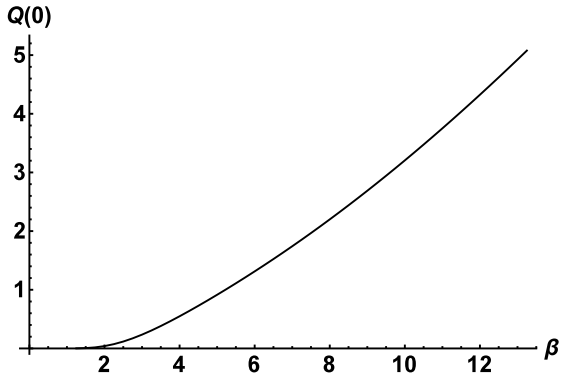

FIG. 1: A plot of the ring closure probability density $Q(\vec{\rho} = \vec{0}) = Q(0)$ versus β, setting $L_P = 1$. It has a small value for short polymers which are hard to bend and form rings and it has a large value for long polymers which are easy to bend and thus the probability density of ring formation is high.

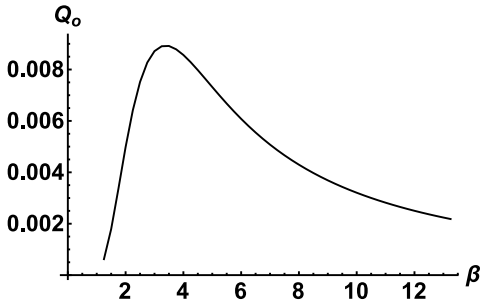

FIG. 2: A plot of the ring closure probability density in physical space $Q_0 = Q(0)/\beta^3$, versus β setting $L_P = 1$. Notice that this function is small for very small and large β and peaks around an intermediate value $\beta \approx 3$.

modes which do not contribute, we find that the contribution from the $x-y$ plane is given by

$$< \phi^2 >^{xy}_{ring} = \frac{1}{12}(1 - \frac{6}{\pi^2})\frac{L}{L_P} \tag{7}$$

We need to add this contribution to the contribution coming from the z direction where the ring closure condition is of the form

$$\int_0^L \phi_z(s) ds = 0.$$

In this case the Fourier expansion for $\phi_z(s)$ can be expressed as $\phi_z(s) = \sum_{n=2}^{\infty} \phi_n e^{\frac{2\pi i n s}{L}}$ which finally gives us

$$< \phi^2 >^{z}_{ring} = \frac{1}{12}(1 - \frac{6}{\pi^2})\frac{L}{L_P} \tag{8}$$

Thus combining Eqs. 7 and 8, the net mean squared tangent angle fluctuation for a three dimensional ring is given by

$$< \phi^2 >^{3d}_{ring} = \frac{1}{6}(1 - \frac{6}{\pi^2})\frac{L}{L_P} \tag{9}$$

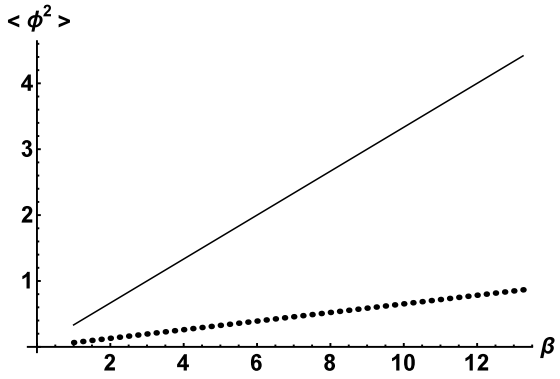

FIG. 3: Plots of mean squared tangent angle fluctuation in three dimensions for a ring (dashed line) and a linear filament (solid line). We have set $L_P = 1$. Notice the suppression of fluctuation for a ring filament compared to a linear one.

A similar calculation for a linear filament in three dimensions gives us

$$< \phi^2 >_{lin}^{3d} = \frac{1}{3}\frac{L}{L_P} \tag{10}$$

We have plotted (9) and (10) in Fig. 3. These predictions can be tested against future experiments on fluorescently tagged actin filaments. Notice that, as in the two dimensional case[5], we find that $< \phi^2 >$ is suppressed for a ringlike structure compared to a linear filament. This indicates that cyclization is entropically costly. Also, as expected, the fluctuations are smaller in the two dimensional geometry compared to the three dimensional geometry.

V. CONCLUSION

Our treatment is an analysis based on the pure bend Worm Like Chain Model. The absence of twist degree of freedom enables our predictions to be directly tested against actin cyclization experiments where the two ends of the polymer come together without any relative twist between the two ends. This is to be contrasted with analysis of J factor of DNA with twist degree of freedom where the additional twist degree of freedom makes the analysis considerably more cumbersome[9–11]. In [11] an interpolation formula is presented in the intermediate rigidity regime. They [11] also presented analytical expressions for the ring closure probability density Q_0 in the limit of $\beta << 1$ and $\beta >> 1$. However, they did not have an exact expression for the entire range of polymer lengths. In contrast, here we present a semianalytical study which gives an essentially exact prediction for Q_0 for the *entire* range of rigidity (See Fig. 1 and Fig. 2). It would be interesting to see how our predictions quantitatively compare with future cyclization probability data for actin filaments. We also expect our predictions for the mean squared tangent angle fluctuation to be tested against future experiments on fluorescently tagged ring like and linear actin filaments in a three dimensional geometry.

ACKNOWLEDGEMENT

One of us (SC) would like to thank RRI for providing hospitality during stay in Raman Research Institute as a Visiting Student.

APPENDIX A: COMPUTATION OF Q_0

Our goal is to calculate Q_0, the ring closure probability. Q_0 is $\tilde{Q}(\vec{r})$ for $\vec{r} = \vec{0}$. $\tilde{Q}(\vec{r})$, the probability distribution for the end to end vector $\vec{r}$ for a semiflexible polymer has the following path integral representation:

$$\tilde{Q}(\vec{r}) = \mathcal{N}\int \mathcal{D}[\hat{t}(s)] exp\{-\frac{1}{k_B T}[\frac{A}{2}\int_0^L (\frac{d\hat{t}}{ds})^2 ds]\} \times \delta^3(\vec{r} - \int_0^L \hat{t} ds) \tag{11}$$

Here $\mathcal{N}$ is the normalization constant and $k_B T$, the thermal energy at temperature T.

Instead of $\tilde{Q}(\vec{r})$ it turns out to be easier to first consider $P(z)$

$$P(z) = \int d\vec{r}\tilde{Q}(\vec{r})\delta(r_3 - z),$$

which is $\tilde{Q}(\vec{r})$ integrated over a plane of constant z.

$P(z)$ in turn is related to $\tilde{P}(f)$, the Laplace transform of $P(z)$ given by:

$$\tilde{P}(f) = \int_{-L}^{L} P(z) e^{\frac{fz}{L_P}} dz \tag{12}$$

f, the variable conjugate to z has the interpretation of a stretching force and thus $\tilde{P}(f)$, can be written as the ratio $Z(f)/Z(0)$ of the partition functions in the presence and absence of an external stretching force f.

$Z(f)$ is given by

$$Z(f) = \mathcal{N}\int \mathcal{D}\left[\hat{t}(s)\right] \exp\left\{-\frac{L_P}{2}\left[\int_o^L \left(\frac{d\hat{t}}{ds}\right)^2 ds\right]\right\} \times \exp\left[\frac{f}{L_P}\int_0^L \hat{t}_2 ds\right]$$

which in turn can be expressed as

$$Z(f) = \mathcal{N}\int \mathcal{D}\left[\hat{t}(\tau)\right] \exp\left\{-\int_o^\beta d\tau \left[\frac{1}{2}\left(\frac{d\hat{t}}{d\tau}\right)^2 - f\hat{t}_z\right]\right\}$$

which has the interpretation of the kernel of a quantum particle on the surface of a sphere at an inverse temperature β. We now exploit the analogy between time imaginary quantum mechanics and classical statistical mechanics to re-express $Z(f)$ as follows:

$$Z(f) = \sum_n e^{-[\beta E_n]} \psi_n\left(\hat{t}_A\right) \psi_n\left(\hat{t}_\beta\right)$$

where $\{\psi_n\left(\hat{t}_A\right)\}$ is a complete set of normalized eigenstates of the Hamiltonian $H_f = -\frac{\nabla^2}{2} - f\cos\theta$ and E_n are the corresponding eigenstates. For free boundary conditions for the end tangent vectors we can express $Z(f)$ as

$$Z(f) = \langle o\,|\exp -\beta H_f|\, o\rangle$$

The Hamiltonian $H_f = -\frac{\nabla^2}{2} - f\cos\theta$ is the Hamiltonian of a rigid rotor in a potential and $|0>$ is the ground state of the free Hamiltonian $H_0 = -\frac{\nabla^2}{2}$. We numerically evaluate $Z(f)$ by choosing a suitable basis in which H_f has a tridiagonal symmetric matrix structure with

$$H_{ll} = \frac{l(l+1)}{2}$$

$$H_{ll+1} = f(l+1)\sqrt{1/[(2l+1)(2l+3)]}$$

To summarize, after casting the problem analytically we use Mathematica programs to sequentially compute $Z(f)$ and $\tilde{P}(f)$, then $P(z)$, then $S(r) = -2rdP(r)/dr = 4\pi r^2\tilde{Q}(r)$ and finally $\tilde{Q}(\vec{r})$. We then consider the scaled variable $\vec{\rho} = \frac{\vec{r}}{\beta}$. $Q(0)$ is then computed by considering $Q(\vec{\rho})$ at $\vec{\rho} = \vec{0}$ and plotting it as a function of β. $Q_0 = \frac{Q(0)}{\beta^3}$. Below we display the programs for computing $Q(\vec{\rho})$ and Q_0. We have inserted some comments as part of the programs for clarity.

Program for computing $Q(\vec{\rho})$

```
ClearAll[h,f,Z,lmax,H,beta,L1,L2,LPR,PR]
lmax=10;
Nmax=3000;
beta=3;
h=.005;
L={};
For[n = 0,n < Nmax + 1,n++,
f=h*n*I;
H = Table[Switch[i - j, -1, f * (i + 1)/Sqrt[
(2i + 1)(2i + 3)], 0, i(i + 1)/2, 1, f * (i)/Sqrt[(2i - 1)(2i +
1)],, 0], i, 0, lmax, j, 0, lmax];
M=MatrixExp[-beta*H];
(*Computation of Z(f)*)
Z=M[[1,1]];
L=Append[L,Z]]
L=Re[L];
Pz={};
P1z={}
For[l=-2,l¡1200,l++,
xi=.001*l;
P=(h*beta/Pi)*Sum[L[[n]]*Cos[(n-
1)*h*xi*beta],n,1,Nmax];
Pz=Append[Pz,xi,P];
P1z=Append[P1z,P]];
V=P1z;
QR1=;
L1=Drop[V,2]
L2=Drop[V,-2]
LPR=(L1-L2)/(.001*2);
LPR=Drop[LPR,1];
(*Computation of S(r)*)
QR = Table[LPR[[i]] * 1/((i - 1) * .001) * [-1/(2 *
Pi)], i, 2, 1199];
(*Computation of Q(r)*)
QR1 = Table[(i - 1) * .001, LPR[[i]] * (1/(i - 1)) *
1/((i - 1) * .001) * [-1/(2 * Pi)], i, 2, 2];
ListPlot[QR1]
```

Program for computing Q_0

```
ClearAll[h, f, Z, lmax, H, beta, Nmax, L1, L2, LPR,
PR]
lmax = 10;
h = .005;
final = {};
For[k = 0, k < 50, k++,
beta = .25*k + 1;
Nmax = Piecewise[90000, beta <= 3, 9000, beta > 3];
L = {};
For[n = 0, n < Nmax + 1, n++, f = h*n*I;
H = Table[Switch[i - j, -1, f * (i + 1)/Sqrt[
(2i + 1)(2i + 3)], 0, i(i + 1)/2, 1, f * (i)/Sqrt[(2i - 1)(2i +
1)],, 0], i, 0, lmax, j, 0, lmax];
M = MatrixExp[-beta*H];
Z = M[[1, 1]];
L = Append[L, Z]]
L = Re[L];
Pz = {};
P1z = {};
For[l = -2, l < 1200, l + +, xi = .001 * l;
P = (h*beta/Pi)*Sum[L[[n]]*Cos[(n - 1)*h*xi*beta], n,
1, Nmax];
Pz = Append[Pz, xi, P];
P1z = Append[P1z, P]];
V = P1z;
QR1 = {};
L1 = Drop[V, 2];
```

L2 = Drop[V, -2];
LPR = (L1 - L2)/(.001*2);
LPR = Drop[LPR, 1];
$QR = Table[LPR[[i]] * 1/((i-1) * .001) * [-1/(2 * Pi)], i, 2, 1199]$;
$QR1 = Table[(i-1) * .001, LPR[[i]] * (1/(i-1)) * 1/((i-1) * .001) * [-1/(2 * Pi)], i, 2, 2]$;
$final = Append[final, beta, (1/beta^3) * QR[[1]]]$
ListPlot[final]

[1] C. Bustamante, S. B. Smith, J. Liphardt, and D. Smith, Current Opinion in Structural Biology **10**(3), 279 (2000), ISSN 0959-440X, URL http://www.sciencedirect.com/science/article/pii/S0959440X00000853.

[2] S. Forth, C. Deufel, M. Y. Sheinin, B. Daniels, J. P. Sethna, and M. D. Wang, Phys. Rev. Lett. **100**(14), 148301 (2008).

[3] B. C. Daniels, S. Forth, M. Y. Sheinin, M. D. Wang, and J. P. Sethna, Phys. Rev. E **80**(4), 040901 (2009).

[4] A. Ott, M. Magnasco, A. Simon, and A. Libchaber, Phys. Rev. E **48**, R1642 (1993), URL http://link.aps.org/doi/10.1103/PhysRevE.48.R1642.

[5] T. Sanchez, I. M. Kulic, and Z. Dogic, Phys. Rev. Lett. **104**, 098103 (2010), URL http://link.aps.org/doi/10.1103/PhysRevLett.104.098103.

[6] M. Mavrakis, T. F.-C. Azou-Gros, Yannick, J. Alvarado, F. Bertin, Aurelie Iv, B. S. Kress, Alla, G. H. Koenderink, and T. Lecuit, Nature Cell Biology **16**, 322 (2014).

[7] J. Samuel and S. Sinha, Phys. Rev. E **66**, 050801 (2002), URL http://link.aps.org/doi/10.1103/PhysRevE.66.050801.

[8] B. Alberts, A. Johnson, J. Lewis, M. Raff, K. Roberts, and P. Walter, *Molecular Biology of the Cell* (Garland Science, 2008).

[9] J. Samuel and S. Sinha, Phys. Rev. Lett. **90**, 098305 (2003), URL http://link.aps.org/doi/10.1103/PhysRevLett.90.098305.

[10] A. J. Spakowitz, EPL (Europhysics Letters) **73**(5), 684 (2006), URL http://stacks.iop.org/0295-5075/73/i=5/a=684.

[11] J. Shimada and H. Yamakawa, Macromolecules **17**, 689 (1984).